Journal of Power Sources 199 (2012) 195–200

Contents lists available at SciVerse ScienceDirect

Journal of Power Sources

journal homepage: www.elsevier.com/locate/jpowsour

Niobium nitride modified AISI 304 stainless steel bipolar plate for proton exchange membrane fuel cell

Lixia Wang, Juncai Sun*, Jing Sun, Ying Lv, Song Li, Shijun Ji, Zhongsheng Wen

Institute of Materials and Technology, Dalian Maritime University, Dalian 116026, China

ARTICLE INFO

Article history:
Received 2 September 2011
Received in revised form 10 October 2011
Accepted 10 October 2011
Available online 15 October 2011

Keywords:
PEMFC
Bipolar plates
Niobium nitride
Interfacial contact resistance
304 Stainless Steel

ABSTRACT

A niobium nitride diffusion coating has been prepared by plasma surface diffusion alloying method on the surface of AISI 304 stainless steel (304 SS) which is applied to bipolar plates for proton exchange membrane fuel cell (PEMFC). The as-prepared niobium nitride diffusion coating consists of a niobium nitride surface layer (8–9 μm) and a Nb and N diffusion solid solution subsurface layer (1–2 μm). The corrosion resistance of the niobium nitride modified 304 SS are investigated and evaluated in simulated PEFMC operating conditions (0.05 M H_2SO_4 + 2 ppm F^- solution at 70 °C). Results show that the niobium nitride diffusion coating greatly improves the corrosion resistance of 304 SS. Self-corrosion potentials of niobium nitride modified 304 SS increase considerably up to 100 mV and 143 mV (vs. SCE) while corrosion current densities remain low at 0.127 μA cm^{-2} and 0.071 μA cm^{-2} in simulated anodic and cathodic environment, respectively. Interfacial contact resistance (ICR) of niobium nitride modified 304 SS is 9.26 mΩ cm^2 under 140 N cm^{-2} compaction force, which is much lower than that of untreated 304 SS, 100.98 mΩ cm^2. After 4 h potentiostatic polarization test, the niobium nitride modified 304 SS exhibits sufficiently low ICR values <20 mΩ cm^2.

1. Introduction

Proton exchange membrane fuel cell (PEMFC) is expected to become a major power source for electrical vehicle and portable applications, due to the following merits: high efficiency, faster startups at room temperature, operating at low temperature (<100 °C), environment friendliness, noiselessness, etc. [1–5]. However, the cost of PEMFC is a significant factor in commercial applications. Among PEMFC components, bipolar plates, a very important multi-functional component, account for the dominant share of the total stack weight and cost [6]. Therefore, bipolar plate is currently one of the main challenges for PEMFC's commercialization. A bipolar plate is used to electrically connect the anode of one single cell to the cathode of adjacent single cell, provide flow fields of reactive gases (hydrogen and oxygen) as well as facilitate water management within the cell in PEMFC stack. Hence, excellent electrochemical corrosion resistance (U.S. Department of Energy target for corrosion rate <1 μA cm^{-2}) and high electrical conductivity (U.S. Department of Energy target for interfacial contact resistance ICR <20 mΩ cm^2 at the compaction force of 140 N cm^{-2}) [7,8] are the foremost prerequisites for the bipolar plate materials used in the PEMFC operating environments with ions F^-, SO_4^{2-}, SO_3^{2-}, HSO_4^-, HSO_3^-, CO_3^{2-}, HCO_3^-, etc. [9–11].

A variety of materials have been chosen and evaluated to serve as PEMFC bipolar plates. Non-porous graphite is the early choice for the bipolar plates for its high conductivity and corrosion resistance. However, graphite's high cost and poor machining property with brittleness are the fatal disadvantages impeding its commercialization. Stainless steels (SS) have been drawn much attention owing to their low prices, good physical and mechanical properties, easy stamping manufacture and thin plate use [12–14]. Nonetheless, the operating conditions of PEMFC are so severe that bare stainless steels cannot be successfully applied into a commercial PEMFC in terms of corrosion resistance and interfacial contact resistance. A lots of surface treatment techniques and methods on stainless steels, including physical vapor deposition (PVD), chemical vapor deposition (CVD), pack cementation, plasma spray, electroplating, electroless plating, sputter deposition, sol–gel dip coating, plasma nitriding and so on [15–20], have been extensively performed to improve their corrosion resistance and electrical conductivity.

Transition metals and their nitrides usually have many attractive characteristics such as high electrical conductivity, good mechanical properties as well as corrosion resistance to chemical attack [21–24]. Multi-arc ion plating TiN was performed on the surface of 316L by Tian et al. [25]. The TiN coated 316L exhibits

* Corresponding author. Tel.: +86 411 84727959; fax: +86 411 84727959.
E-mail address: sunjc@dlmu.edu.cn (J. Sun).

0378-7753/$ – see front matter © 2011 Elsevier B.V. All rights reserved.
doi:10.1016/j.jpowsour.2011.10.034

improved corrosion resistance and promising ICR, but in that work, the long-term stability of TiN coating had not been mentioned. In general, the TiN coating prepared by physical vapor deposition (PVD) methods has inherent pinhole or micro-pore defects [26–28], which have influence on the stability of passive region on polarization curves and degrade the durability of coating layer in corrosion environments. Sun's group [14,20] suggested a plasma nitriding method to form dense surface layer of nitrogen supersaturated austenite (γ_N) phase on austenite stainless steels, such as AISI 316L and 304L. The γ_N phase provides better corrosion resistance and lower ICR than untreated stainless steels. After electrochemical polarization, the ICRs of plasma nitrided 316L are in the range of 100–300 mΩ cm^2 at the compaction force of 150 N cm^{-2} and seem to be unacceptable for the bipolar plate use. Brady et al. [29] reported that the corrosion resistance of Ni–50Cr alloy was improved by thermal (gas) nitridation at 1100 °C, and the ICR was low before and after polarization. This Ni–50Cr alloy is too expensive to use, except of special applications. However, a discontinuous and porous nitride layer formed on the surface of stainless steel 349^{TM} by thermal nitridation leads to the high passive current density both in anodic and cathodic conditions [30], yet, nitrided AISI446 shows improved corrosion resistance and lower ICR for the 2 h nitrided sample with nitrogen modification of the native passive oxide layer, however, poor corrosion resistance for the 24 h nitrided one with discontinuous inward-growing $(Cr, Fe)_2N_{1-x}$ nitride layer [31]. A composite method of electroplating Cr and heat-diffusion treatment was adopted by Wang et al. [32] and a dense, continuous high chromium layer with about 10 μm thickness was formed on the surface of AISI 304 SS. Though the high Cr layer possesses better corrosion resistance than the untreated sample, ICR is far from satisfactory and a further modification is needed for lowering the ICR. Nam et al. [33] nitrided the electroplated Cr on the surface of AISI 316L and obtained a more preferable Cr_2N film than CrN + Cr_2N blended coating through controlling the nitriding conditions. The Cr_2N layer grown by thermal nitridation of the electroplated chromium layer exhibits lowered ICR and improved corrosion resistance. However, this Cr_2N layer must be obtained by two separate steps in different facilities, increasing the preparing complexity and cost accordingly. Niobium in stainless steels is a very important alloying element to upgrade intergranular corrosion resistance and stabilization in the case of sulfuric and hydrochloric acid solutions [34,35]. Weil et al. [36] fabricated a niobium external cladding layer (50 μm thick) on 430 SS sheet by roll cladding method, and the well properties of niobium, such as high conductivity as well as perfect corrosion resistance, had been successfully transplanted to the 430 SS substrate. Nonetheless, the cost of the thick Nb cladding layer is expensive and the thickness reduction of Nb cladding layer is difficult.

Niobium nitrides were initially fabricated as a film for superconductor application by various deposition methods, such as ion beam assisted deposition [22], reactive magnetron sputtering [37], filtered arc deposition [38], pulsed laser deposition [39] and vacuum arc deposition [40]. The mechanical and physical–chemical properties of niobium nitrides, for instance, wear resistance, crack resistance, microhardness [41,42], high temperature stability [43] and corrosion resistance [44] have been widely investigated for mechanical structure applications. In our present work, niobium nitrides were applied and expected to improve corrosion resistance and surface electrical conductivity of the stainless steel bipolar plates in PEMFC. The niobium nitrides were prepared by plasma surface diffusion alloying method on the surface of AISI 304 stainless steel (304 SS) and the corrosion resistance and surface electrical conductivity of the niobium nitride modified 304 SS (hereinafter referred as Nb–N 304 SS) were tested and evaluated in simulated PEMFC environments.

2. Experimental

2.1. Specimen preparation

Commercial 304 SS sheets (thickness 1.5 mm) were cut into specimens of 10 mm × 10 mm via an Electric Discharge Machining (EDM). The surface of every specimen was in turn ground with SiC papers from #360 up to #1500 grit and polished mechanically with diamond paste and then degreased with acetone in an ultrasonic cleaner and lastly dried at room temperature.

The niobium nitride diffusion coating was formed on the surface of 304 SS in the following consecutive two steps in a double glow plasma alloying furnace, which has three electrodes: an anode, a negative cathode (specimens) and a sputtering source cathode (Nb sinter plate). In step 1: the specimens were firstly heated at 1173 K by work power supply and particle bombardment in the chamber filled with pure Ar to clean the specimen surface at the pressure of 40 Pa and bias voltage of −1 kV. By keeping specimens at 1173 K, then, the source electrode power supply was loaded and kept at −800 to −900 V, meanwhile the bias voltage of specimens was decreased to −530 to −580 V, which can allow more alloy sputtering elements to move from the source electrode into the surface of specimens. Specimens were treated at 1173 K for 2 h as a niobium diffusion process at high temperatures. And in the consequent step 2, proportional Ar and nitrogen (N_2) mixed gases (Ar:N_2 = 10:1–8:1) were introduced to produce a niobium nitride modified layer at 1173 K for another 2 h, meanwhile all the other processing parameters were kept the same as step 1's. After plasma surface niobium nitride diffusion alloying processing, scanning electron microscopy (SEM) in combination with energy-dispersive X-ray Spectrometer (EDS) as well as X-ray diffraction (XRD) was used to observe and analyze the surface modified layer of specimens.

2.2. Electrochemical measurements

Potentiodynamic and potentiostatic tests were performed to measure the corrosion resistance of the bare and modified specimens, respectively. A sulfuric acid solution (0.05 M H_2SO_4 + 2 ppm F^- solution) at 70 °C [9–11] was used as an electrolyte in order to simulate the aggressive PEMFC environment. Prior to each test, specimens were cleaned with ethanol then embedded in corrosion test cells. The corrosion test cell is constructed with PTFE material to fix and seal specimen as well as ensure only one side of the specimen contacting with the test solution for electrochemical measurements. The electrochemical measurements were conducted in a CHI660C electrochemical workstation controlled by a computer. A conventional three-electrode system was used for the electrochemical measurements, with a platinum sheet as the counter electrode and a saturated calomel electrode (SCE) connected to a Luggin capillary as the reference electrode. All the potentials reported are relative to SCE unless noted. The temperature of the corrosion test was maintained by an isothermal bath during electrochemical tests.

The potentiodynamic tests were carried out to investigate general polarization behavior of these specimens. Before corrosion tests, all the specimens were stabilized at open circuit potential for 30 min, and then started the potential sweep from a specific voltage, below 0.2 V of the open circuit voltage, at a scanning rate of 1 mV s^{-1}. In actual PEMFC working conditions, the operating voltage of single-cell is chosen as 0.7 V and the anode potential is corresponded to −0.1 V_{SCE} while the cathode potential is corresponded to 0.6 V_{SCE} [45]. Therefore, when potentiostatic tests were performed in simulated anodic environment, the applied potential was −0.1 V (vs. SCE) with H_2 purging and in simulated cathodic environment, the applied potential was 0.6 V (vs. SCE) with air purging.

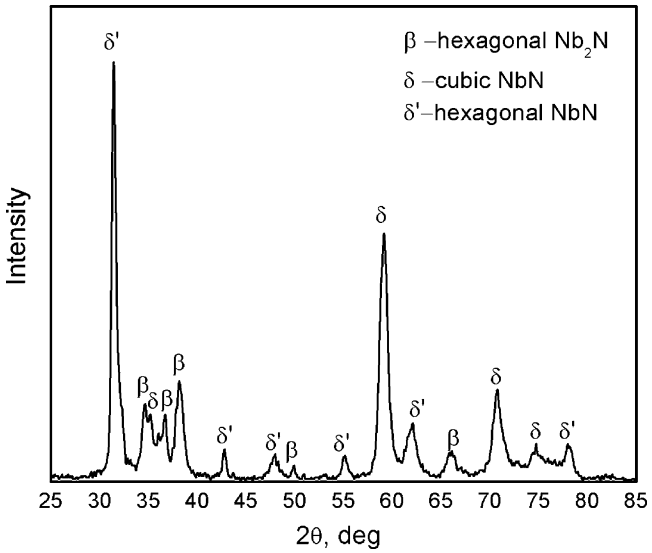

Fig. 1. X-ray diffraction pattern of niobium nitride diffusion coating.

2.3. Interfacial contact resistance (ICR)

The method described in Ref. [46] was applied to measure ICR under different compaction forces. The specimen was sandwiched between two carbon papers (Toray, Inc.) and the carbon paper/specimen/carbon paper sandwich was further put into two copper plates for force loading. In order to reduce the thermal effect of the current, a constant current (100 mA) provided by an YJ-10A type galvanostat was used via two copper plates. Steadily increased compaction forces were obtained through screwing a screw nut and a lead screw whose records were kept by a MCK-C compaction sensor, a special force gauge. Meanwhile the variable potentials were recorded by a Solartron 7081 digital voltmeter (precision 10^{-8} V).

3. Results and discussion

3.1. Characteristics of the niobium nitride diffusion layer

The X-ray diffraction (XRD) was carried out to identify the crystal structure of the niobium nitride diffusion coating and the XRD spectra are shown in Fig. 1. According to the Joint Committee on Powder Diffraction Standards (JCPDS) cards, the niobium nitrides of hexagonal β-Nb_2N (space group $P6_3/mmc$, prototype Fe_2N), hexagonal δ′-NbN (space group $P6_3/mmc$, prototype NiAs) and cubic δ-NbN (space group Fm-3m, prototype, NaCl) phases are identified in the XRD pattern. It is assumed, from these results, that the niobium nitride diffusion coating has multi-phases of β-Nb_2N, δ′-NbN and δ-NbN.

From the cross-sectional view of the niobium nitride modified 304 SS shown in Fig. 2(a), it is apparent that the niobium nitride diffusion coating is uniform in thickness (about 10 μm), dense in microstructures without pinhole, micropore and microcracks, and well in metallurgical adhesion to the 304 SS substrate with no interfacial defects. Fig. 2(b) shows the elemental linear scanning pattern of niobium, nitrogen, iron, chromium and nickel across the niobium nitride diffusion coating. It can be seen that there exists a niobium nitride surface layer with thickness of ~9 μm as well as an Nb and N diffusion solid solution subsurface layer (about 1 μm in thickness) on the modified surface of 304 SS. However, as the back scattering electron micrograph shown in Fig. 2(a) the niobium nitride diffusion coating seems to be a multilayer structure. According to the Nb–N binary phase diagram, both Nb_2N and NbN phase layers may appear successively during a reactive diffusion process. In our results, more than two layers in the coating were formed, implying the formation process of niobium nitride diffusion coating is affected by both the diffusion and deposition function simultaneously. The study on the structure and composition of the multilayer film coating and the formation mechanisms are still underway.

3.2. Corrosion resistance

The potentiodynamic curves for untreated and Nb–N 304 SS are measured in 0.05 M H_2SO_4 + 2 ppm F^- solution at 70 °C purged with H_2 to simulate the anodic environment (Fig. 3(a)) or purged with air to simulate the cathodic environment (Fig. 3(b)), respectively. All the studied specimens show passivation zone. For the untreated 304 SS, a high peak of active–passive transitions appears on polarization curves in both anodic and cathodic evironments. However, the polarization curves of Nb–N 304 SS in both anodic and cathodic environment almost turn directly into passivation along with the rising of potential without obviously active–passive transition, which indicate that the Nb–N 304 SS can be self-passivated. Meanwhile, the corrosion potential E_{corr} of Nb–N 304 SS shifts markedly to positive direction by contrast to the untreated 304 SS both in simulated anodic and cathodic environment. In the anodic environment purged with H_2, E_{corr} of the untreated 304 SS is close to −347 mV while E_{corr} of the Nb–N 304 SS is close to 100 mV, and the same tendency appears in the cathodic environment purged with air. E_{corr} is situated at −319 mV and 143 mV for the untreated and Nb–N 304 SS, respectively. The corrosion current density I_{corr}

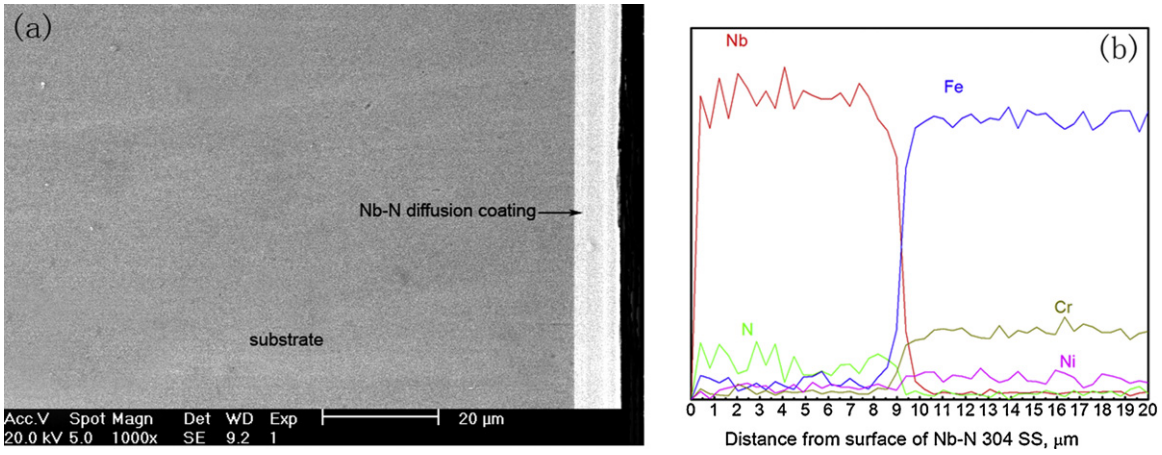

Fig. 2. (a) SEM micrographs of cross-section for Nb–N 304 SS. (b) Elemental EDS analysis for niobium nitride diffusion coating.

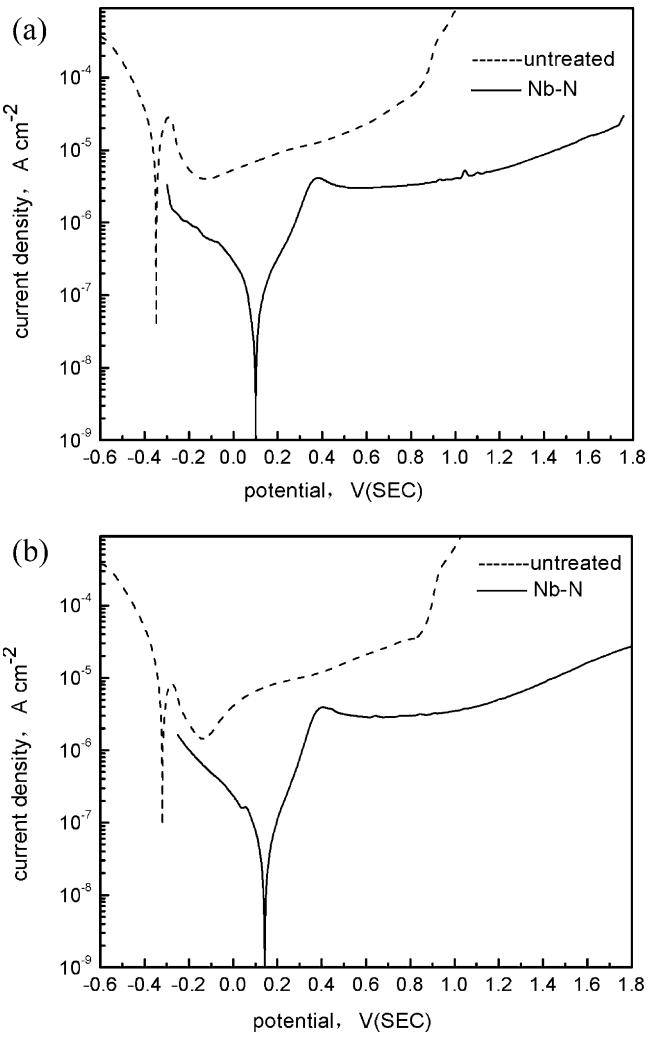

Fig. 3. Potentiodynamic polarization curves of untreated and Nb–N 304 SS in 0.05 M H_2SO_4 + 2 ppm F^- solution at 70 °C purged with air (a) and H_2 (b).

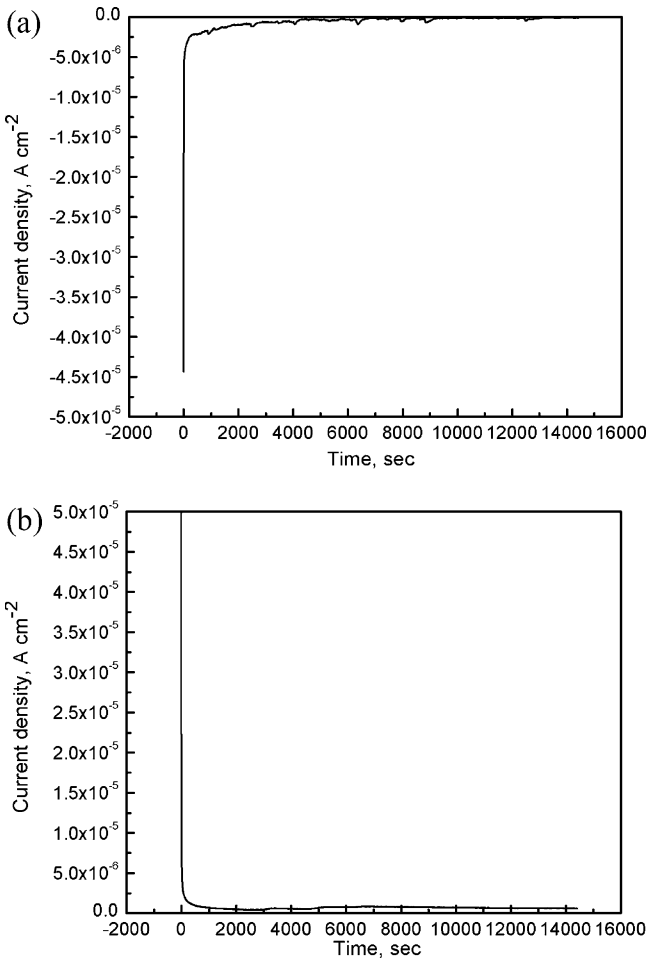

Fig. 4. Current density–time relationship of Nb–N 304 SS in 0.05 M H_2SO_4 + 2 ppm F^- solution at 70 °C purged with H_2 (a) and air (b).

was also obtained by linear-polarization method. The results are shown in Table 1. It can be clearly seen that the I_{corr} of Nb–N 304 SS decrease obviously in simulated PEMFC environment and corrosion rates are more than one order of magnitude lower than those of the untreated ones.

According to the aforementioned potentiodynamic results, the I_{corr} of the untreated 304 SS are still very high and the passive film formed on its surface cannot be competent as the protective layer for untreated 304 SS in the bipolar plate application, although an obvious passive region occurs in the simulated PEMFC environment. Compared to the untreated 304 SS, the Nb–N 304 SS have a significant decrease in the I_{corr} in simulated PEMFC environment, which demonstrates that the corrosion resistance of the Nb–N 304 SS is greatly ameliorated. The improvement is attributed to the dense niobium nitride diffusion coating formed on the surface of 304 SS, which protects the 304 SS substrate from corrosion of the sulfuric acid solution in simulated PEMFC environment.

The long-term stability of Nb–N 304 SS was studied by potentiostatic polarization in simulated PEMFC environment for 4 h. As aforementioned, in actual working conditions of PEMFC, the anode potential is at $-0.1\,V_{SCE}$ while the cathode potential is at $0.6\,V_{SCE}$. Therefore, the bipolar plates undergo corrosion at an applied potential which is different from the free potential corrosion. Fig. 4(a) and (b) shows the potentiostatic polarization results of the Nb–N 304 SS under applied potential of $-0.1\,V_{SCE}$ with H_2 purging and $0.6\,V_{SCE}$ with air purging, respectively. From Fig. 4(a), which is in the simulated anodic environment, we can see that the current density of Nb–N 304 SS is negative in the whole test process and finally stabilizes at $-(0.8–4)\times10^{-7}\,A\,cm^{-2}$. The negative current density is attributed to the reduction of H^+ ions that changes to H_2 and provides cathodic protection for the Nb–N 304 SS. Additionally, under the cathodic protection the active dissolution rate of Nb–N 304 SS is quite low in the simulated anodic environment. Fig. 4(b) presents potentiostatic testing in simulate cathodic environment, it can be seen that current density decays rapidly at the initial stage of potentiostatic polarization and then stabilizes at $(2–8)\times10^{-7}\,A\,cm^{-2}$ in the following stage. Although the

Table 1
Corrosion current density of untreated and Nb–N 304 SS polarized in simulated PEMFC conditions.

Specimen	Purged with H_2		Purged with air	
	I_{corr} ($\mu A\,cm^{-2}$)	E_{corr} ($mV_{vs.\,SCE}$)	I_{corr} ($\mu A\,cm^{-2}$)	E_{corr} ($mV_{vs.\,SCE}$)
Untreated 304 SS	21.204	−347	13.453	−319
Nb–N 304 SS	0.127	100	0.071	143

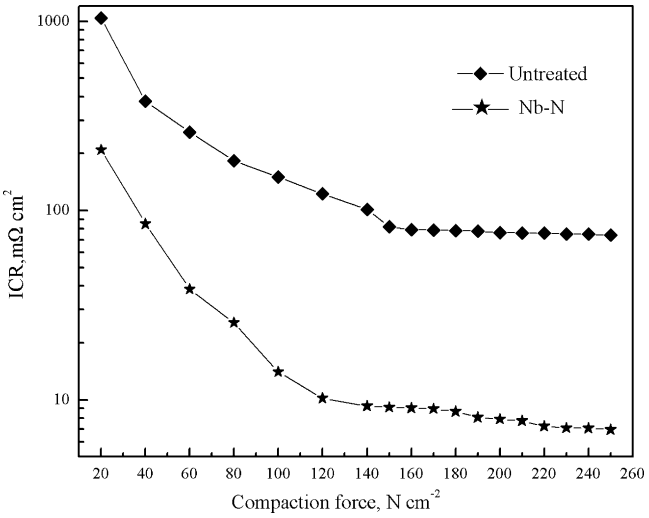

Fig. 5. Interfacial contact resistance ICR of untreated 304 SS $R_{C/SS}$ and Nb–N 304 SS $R_{C/Nb}$ with compaction force.

positive current density obtained from the potentiostatic testing under cathodic environment demonstrates a slight corrosion of the Nb–N 304 SS undergoing, the quite low stable current density illustrates the good corrosion resistance of niobium nitride diffusion coating possessing. No deterioration is observed during potentiostatic testing, as is evidenced by the absence of the obvious current density fluctuation in the polarization curves, suggesting the niobium nitride diffusion coating is quite stable at both the anodic and cathodic working potential of PEMFC.

3.3. Interfacial contact resistance (ICR)

The ICR between carbon paper and specimen is expressed as $R_{C/S}$. Fig. 5 shows the relationship between ICR of untreated ($R_{C/SS}$) and Nb–N 304 SS ($R_{C/Nb}$) and variable compaction force. It is observed that ICRs reduce rapidly with the compaction forces increased at first, and then become stable gradually when the compaction force reaches more than 100 N cm^{-2}. As the effective contact area between the carbon paper and the 304 SS gradually achieves the maximum, the compaction force is no longer the dominant influence on the ICR. In the whole measurement range $R_{C/Nb}$ is evidently lower than $R_{C/SS}$ at the same compaction force owing to the higher conductivity of the niobium nitride diffusion coating prepared by plasma surface diffusion alloying method. When the compaction force reaches to 140 N cm^{-2}, $R_{C/Nb}$ is 9.26 mΩ cm^2 far lower than that of the untreated 304 SS ($R_{C/SS}$ 100.98 mΩ cm^2) with air-formed oxide film. The air-formed oxide film on stainless steel, as well known, is generally dominant of prior Cr_2O_3 forming, which is a semiconductor oxide to result in the higher ICR than niobium nitride.

When the material is used as bipolar plate of PEMFC, the aggressive acid and specific electrode potential operating condition must be undertaken and the surface of materials is attacked corrosively or passivated. In this circumstance, a passive film will be expected to be formed and stabilized on the surface of stainless steel. Although this passive film prevents the substrate from further corrosion, it increases surface resistance and accordingly results in degradation of the PEMFC performance. So it is essential to measure the relationship between variable compaction force and ICR of untreated and Nb–N 304 SS after potentiostatic polarization, as shown in Fig. 6(a) and (b). Both ICRs of untreated and Nb–N 304 SS have increased after potentiostatic polarization for 4 h at operation potential in simulated PEMFC environment. Unlike the significantly

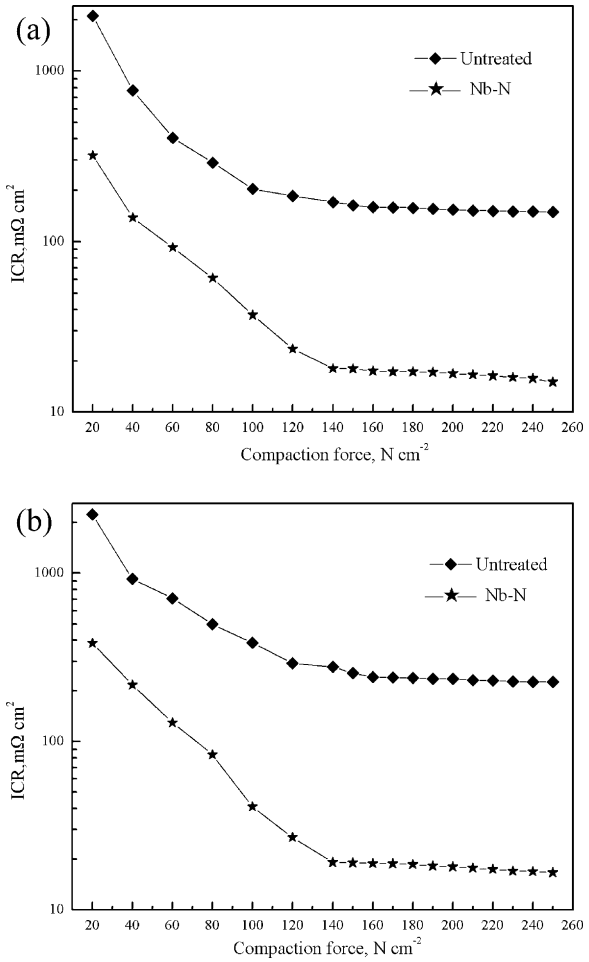

Fig. 6. Interfacial contact resistance ICR of untreated 304 SS $R_{C/SS}$ and Nb–N 304 SS $R_{C/Nb}$ with compaction force after potentiostatic testing in simulated anodic (a) and cathodic (b) environment.

increased $R_{C/SS}$, the magnitudes of the increased $R_{C/Nb}$ are small. At the compaction of 140 N cm^{-2}, $R_{C/SS}$ is about 170.52 mΩ cm^2 while $R_{C/Nb}$ is about 18.02 mΩ cm^2 after potentiostatic polarization in anodic environment; and $R_{C/SS}$ is about 278.25 mΩ cm^2 while $R_{C/Nb}$ is about 19.14 mΩ cm^2 after potentiostatic polarization in cathodic environment. Therefore, though the surface resistance ICR of Nb–N 304 SS increases a little, the niobium nitride diffusion coating keeps stable and lower ICR in simulated PEMFC conditions.

4. Conclusions

Niobium nitride diffusion coating with thickness about 10 μm is fabricated on the surface of 304 SS through the plasma surface diffusion alloying method. Microstructure of the coating is a dense multilayer with uniformed thickness, and well bonding metallurgically with the substrate. The corrosion resistance and conductivity of niobium nitride diffusion coating as a protective layer on 304 SS bipolar plate were evaluated in simulated PEMFC environments. The Nb–N 304 SS has shown excellent passivated behavior and considerably improved corrosion resistance in simulated PEMFC operating condition in comparison with the untreated ones. Moreover, the niobium nitride diffusion coating is very stable during 4 h potentiostatic test both in simulated anodic and cathodic environment. Interfacial contact resistance of Nb–N 304 SS is 9.26 mΩ cm^2 under 140 N cm^{-2} compaction force, which is much lower than that of untreated 304 SS (100.98 mΩ cm^2). After 4 h potentiostatic test, though the ICRs show a little increase, the Nb–N 304 SS exhibits

sufficiently low ICR values. Therefore, the Nb–N 304 SS is promising to be used as bipolar plates for proton exchange membrane fuel cells.

Acknowledgement

This work is financially supported by the National Foundation of Natural Science of China (Nos. 20776022 and 21176034).

References

[1] C.E. Borroni-Bird, J. Power Sources 61 (1996) 33–48.
[2] S.G. Chalk, J.F. Miller, F.W. Wagner, J. Power Sources 86 (2000) 40–45.
[3] P. Costamagna, S. Srinivasan, J. Power Sources 102 (2001) 242–252.
[4] C. Song, Catal. Today 77 (2002) 17–49.
[5] S. Gamburzev, A.J. Appleby, J. Power Sources 107 (2002) 5–12.
[6] H. Tsuchiya, O. Kobayashi, Int. J. Hydrogen Energy 29 (2004) 985–990.
[7] R.A. Antunes, M.C.L. Oliveira, G. Ett, V. Ett, Int. J. Hydrogen Energy 35 (2010) 3632–3647.
[8] H. Tawfik, Y. Hung, D. Mahajan, J. Power Sources 163 (2007) 755–767.
[9] Y. Li, W. Meng, S. Swathirajan, S. Harris, G. Doll, US Patent 5624769, 1997.
[10] J.K. Neutzler, US Patent 5776624, 1998.
[11] R. Hornung, G. Kappelt, J. Power Sources 72 (1998) 20–21.
[12] R.J. Tian, J.C. Sun, J. Power Sources 194 (2009) 981–984.
[13] R.J. Tian, J.C. Sun, J.L. Wang, Rare Metals Vol. 25 (October) (2006) 229 (special issue).
[14] R.J. Tian, J.C. Sun, L. Wang, J. Power Sources 163 (2007) 719–724.
[15] S.J. Lee, C.H. Huang, Y.P. Chen, J. Mater. Process. Technol. 140 (2003) 688–693.
[16] A. Heinzel, F. Mahlendorf, O. Niemzig, C. Kreuz, J. Power Sources 131 (2004) 35–40.
[17] H. Wang, J.A. Turner, J. Power Sources 170 (2007) 387–394.
[18] W.G. Lee, K.H. Cho, S.B. Lee, S.B. Park, H. Jang, J. Alloys Compd. 474 (2009) 268–272.
[19] C.Y. Chung, S.K. Chen, P.J. Chiu, M.H. Chang, T.T. Hung, T.H. Ko, J. Power Sources 176 (2008) 276–281.
[20] R.J. Tian, J.C. Sun, L. Wang, Int. J. Hydrogen Energy 31 (2006) 1874–1878.
[21] W.S. Williams, Int. J. Refract. Met. Hard. Mater. 17 (1999) 21–26.
[22] W. Ensinger, Nucl. Instrum. Methods Phys. Res. Sect. B 106 (1995) 142–146.
[23] K.S. Havey, J.S. Zabinski, S.D. Walck, Thin Solid Films 303 (1997) 238–245.
[24] N. Hayashi, I.H. Murzin, I. Sakamoto, M. Ohkubo, Thin Solid Films 259 (1995) 146–149.
[25] R.J. Tian, J.C. Sun, Int. J. Hydrogen Energy 36 (2011) 6788–6794.
[26] H.C. Barshilia, M.S. Prakash, A. Poojari, K.S. Rajam, Thin Solid Films 460 (2004) 133–142.
[27] Y. Wang, D.O. Northwood, Int. J. Hydrogen Energy 32 (2007) 895–902.
[28] Y. Wang, D.O. Northwood, J. Power Sources 165 (2007) 293–298.
[29] M.P. Brady, K. Weisbrod, I. Paulauskas, R.A. Buchanan, K.L. More, H. Wang, M. Wilson, F. Garzon, L.R. Walker, Scripta Mater. 50 (2004) 1017–1022.
[30] H. Wang, M.P. Brady, G. Teeter, J.A. Turner, J. Power Sources 138 (2004) 86–93.
[31] H. Wang, M.P. Brady, K.L. More, H.M. Meyer III, J.A. Turner, J. Power Sources 138 (2004) 79–85.
[32] J.L. Wang, J.C. Sun, S. Li, Z.S. Wen, S.J. Ji, Int. J. Hydrogen Energy (2011), doi:10.1016/j.ijhydene.2011.02.072.
[33] D.G. Nam, H.C. Lee, J. Power Sources 170 (2007) 268–274.
[34] H. Demiroren, J. Appl. Electrochem. 39 (2009) 761–767.
[35] A. Robin, Int. J. Refract. Met. Hard. Mater. 15 (1997) 317–323.
[36] K.S. Wei, G. Xia, Z.G. Yang, J.Y. Kim, Int. J. Hydrogen Energy 32 (2007) 3724–3733.
[37] S.K. Kim, B.C. Cha, J.S. Yoo, Surf. Coat. Technol. 177–178 (2004) 434–440.
[38] A. Bendavid, P.J. Martin, T.J. Kinder, E.W. Preston, Surf. Coat. Technol. 163–164 (2003) 347–352.
[39] G. Cappucio, U. Gambardella, A. Morone, S. Orlando, G.P. Parisi, Appl. Surf. Sci. 109 (1997) 399–402.
[40] V.N. Zhitomirsky, I. Grimberg, L. Rapoport, N.A. Travitzkyd, R.L. Boxmana, S. Goldsmitha, A. Raihel, I. Lapsker, B.Z. Weiss, Thin Solid Films 326 (1998) 134–142.
[41] M. Larsson, P. Hollman, P. Hendequist, S. Hogmark, U. Wahlstrom, L. Hultman, Surf. Coat. Technol. 86–87 (1996) 351–356.
[42] V.N. Zhitomirsky, I. Grimberg, L. Rapoport, N.A. Travitzky, R.L. Boxman, S. Goldsmith, A. Raihelc, I. Lapsker, B.Z. Weiss, Thin Solid Films 326 (1998) 134–142.
[43] I. Hotovy, D. Buc, J. Brcka, R. Srnanek, Phys. Status Solidi A 161 (1997) 97–104.
[44] M. Fenker, M. Balzer, H.A. Jehn, H. Kappl, J.J. Lee, K.H. Lee, H.S. Park, Surf. Coat. Technol. 150 (2002) 101–106.
[45] R.L. Borup, N.E. Vanderborgh, Mater. Res. Soc. 393 (1995) 151.
[46] H. Wang, M.A. Sweikart, J.A. Turner, J. Power Sources 115 (2003) 243–251.